




Ligand concentration-dependent supramolecular complexes with uncoordinated carbonyl groups based on a new pyrazole carboxylic acid ligand

Qinghong Xia, Yanqiu Ren, Mei-Ling Cheng, Xiuxiu Liu, Sheng Chen, Changwei Zhai & Qi Liu


To cite this article: Qinghong Xia, Yanqiu Ren, Mei-Ling Cheng, Xiuxiu Liu, Sheng Chen, Changwei Zhai & Qi Liu (2015) Ligand concentration-dependent supramolecular complexes with uncoordinated carbonyl groups based on a new pyrazole carboxylic acid ligand, Journal of Coordination Chemistry, 68:10, 1688-1704, DOI: [10.1080/00958972.2015.1020305](https://doi.org/10.1080/00958972.2015.1020305)

To link to this article: <http://dx.doi.org/10.1080/00958972.2015.1020305>

 View supplementary material 

 Accepted author version posted online: 18 Feb 2015.
Published online: 24 Mar 2015.

 Submit your article to this journal 

 Article views: 62

 View related articles 

 View Crossmark data 

 Citing articles: 1 View citing articles 

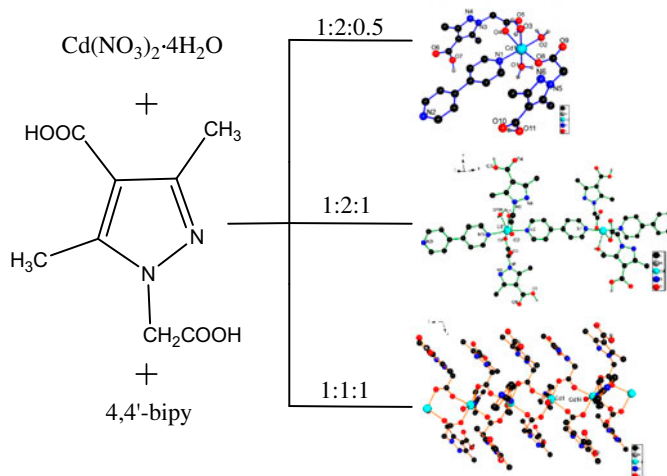
Ligand concentration-dependent supramolecular complexes with uncoordinated carbonyl groups based on a new pyrazole carboxylic acid ligand

QINGHONG XIA†, YANQIU REN†, MEI-LING CHENG‡, XIUXIU LIU†, SHENG CHEN†, CHANGWEI ZHAI† and QI LIU*†‡

†School of Petrochemical Engineering and Jiangsu Key Laboratory of Advanced Catalytic Materials and Technology, Changzhou University, Changzhou, China

‡State Key Laboratory of Coordination Chemistry, Nanjing University, Nanjing, China

(Received 15 October 2014; accepted 29 January 2015)



One new ligand, (H₂cmdpca), and three supramolecular complexes, [Cd(4,4'-bpy)(Hcmdpca)₂(H₂O)₃]·H₂O (**1**), [Cd(4,4'-bpy)(Hcmdpca)₂(H₂O)]·3H₂O (**2**), and [Cd(4,4'-bpy)(Hcmdpca)₂(H₂O)] (**3**), have been synthesized and characterized.

One new pyrazole-based ligand, 1-carboxymethyl-3,5-dimethyl-1H-pyrazole-4-carboxylic acid (H₂cmdpca), has been synthesized and characterized. Structural analysis reveals that H₂cmdpca crystallizes in the monoclinic system and adopts a 3-D supramolecular network via the interaction of intermolecular hydrogen bonds. The reactions of Cd(II) ions with H₂cmdpca and 4,4'-bipyridine (4,4'-bpy) afforded three metal complexes, [Cd(4,4'-bpy)(Hcmdpca)₂(H₂O)₃]·H₂O (**1**), [Cd(4,4'-bpy)(Hcmdpca)₂(H₂O)]·3H₂O (**2**), and [Cd(4,4'-bpy)(Hcmdpca)₂(H₂O)] (**3**). Structural analyses reveal that these complexes are all monoclinic and **1**, **2**, and **3** exhibit mononuclear, 1-D chain, and 1-D with binuclear loop structures, respectively, which are further assembled into 3-D supramolecular

*Corresponding author. Emails: liuqi62@163.com, liuqi@cczu.edu.cn

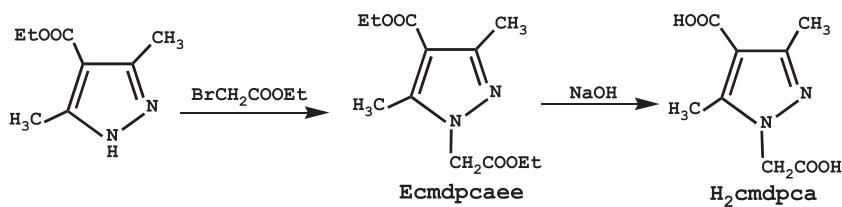
frameworks through non-covalent interactions. **1** and **2** are true supramolecular isomers, while **2** and **3** are “pseudo-supramolecular” isomers. In addition, the thermal stability and luminescent properties of the complexes are also investigated.

Keywords: N-Heterocyclic ligand; Cadmium(II); Crystal structure; Photoluminescence; Supramolecular isomers

1. Introduction

The design and synthesis of supramolecular complexes and coordination polymers have attracted interest owing to their topologically diverse structures [1, 2] and potential applications in catalysis [3, 4], gas storage and separation [5–8], sensors [9], lithium-ion batteries [10–12], magnetic and optical properties, etc. [13–15]. Self-assembly of supramolecular complexes is influenced by various factors such as organic ligands, metal ions, solvent systems, metal ion to ligand molar ratio, pH, etc. While the selection of ligands plays a key role in assembling coordination polymers, slight change of the ligands, such as symmetry, flexibility, and the number of coordinated atoms, may result in dramatic differences in structures and properties. Reported coordination polymers of organic N-heterocyclic carboxylic acid ligands, such as pyrazolecarboxylic acid [16–27] and imidazolecarboxylic acid [28], are frequently chosen to fabricate various topological frameworks for their rich coordination modes and/or flexible configurations. In order to expand the study in this field, we synthesized a new ligand, 1-carboxymethyl-3,5-dimethyl-1H-pyrazole-4-carboxylic acid ($H_2cmdpca$) (scheme 1), for the following reasons: (1) lack of symmetry in the positioning of carboxylate groups in the ligand, $-COOH$ and $-CH_2COOH$ benefit structural tunability; (2) because $H_2cmdpca$ can be partially or fully deprotonated to generate $Hcmdpca^-$ and $cmdpca^{2-}$ at different pH values, and has a rigid N-heterocyclic ring and a flexible $-CH_2COOH$ spacer, it may have different coordination modes when coordinating to metal ions, and diverse structures, such as supramolecular isomers.

Supramolecular isomerism has gained considerable attention in crystal engineering and supramolecular chemistry to help understand the factors that control and influence crystal growth and the relationship between the structures and properties of structural isomers [29–31]. Most supramolecular isomers belong to a group of solvent-induced (guest-induced) pseudo-polymorphism [32–42]. Recently, true supramolecular isomers with fixed stoichiometry for all components, which lie at the very heart of the concept of supramolecular isomerism, have received attention [43–55]. However, synthesis of true supramolecular isomers is still a formidable task. Some strategies for synthesizing true supramolecular



Scheme 1. The synthetic process of Ecmdpcae and $H_2cmdpca$.

isomers, such as template/additive-induced synthesis [48, 54, 55] and temperature-controlled synthesis [45], have been studied, but only a few true supramolecular isomers obtained via metal–ligand molar ratio/ligand concentration-controlled synthesis have been reported [49]. Examples of true and “pseudo-supramolecular” isomers obtained at the same time only by changing the ligand concentration have not been reported. With the aforementioned consideration, and also as continuation of our previous efforts in constructing functional coordination polymers [10], we adopted the extensively studied neutral nitrogen donor ligand 4,4'-bipyridine (4,4'-bpy), as coligand to react with H₂cmdpca and cadmium salt in different molar ratios. Three supramolecular complexes containing uncoordinated carbonyl groups were obtained, [Cd(4,4'-bpy)(Hcmdpca)₂(H₂O)₃]·H₂O (**1**), [Cd(4,4'-bpy)(Hcmdpca)₂(H₂O)]·3H₂O (**2**), and [Cd(4,4'-bpy)(Hcmdpca)₂(H₂O)] (**3**). Compounds **1** and **2** are true supramolecular isomers, while **2** and **3** have the same building blocks but different network superstructures and can be related as “pseudo-supramolecular” isomers. Furthermore, structural characterization and fluorescence of H₂cmdpca, and thermal stability and fluorescence properties of the complexes have also been studied.

2. Experimental

2.1. Materials and instruments

All reagents and solvents were used as received from commercial sources. 3,5-Dimethyl-1H-pyrazole-carboxylic acid ethyl ester was prepared according to the literature [56]. NMR spectra were recorded on a Bruker DRX500 (500 and 400 Hz for ¹H). Single-crystal X-ray determinations of H₂cmdpca, **1**, **2**, and **3** were performed on a Bruker SMART CCD diffractometer at 291(2) K (**1**, **2**, and **3**). The elemental analyses (C, H, and N) were performed with a Perkin-Elmer 2400 Series II element analyzer. IR spectra were recorded on a Nicolet 460 spectrometer using KBr pellets from 4000 to 400 cm⁻¹. Electrospray mass spectra (ESI-MS) were carried out by a Shimadzu GCMS-QP2010 ion trap mass spectrometer. The luminescence spectra of solid samples were recorded with a Varian Cary Eclipse spectrometer. Thermogravimetric analysis experiments were carried out on a DuPont thermal analyzer from room temperature to 800 °C under N₂ at a heating rate of 10 °C min⁻¹.

2.2. Synthesis

2.2.1. Synthesis of 1-ethoxycarbonylmethyl-3,5-dimethyl-1H-pyrazole-4-carboxylic acid ethyl ester (Ecmdpcaee). 3,5-Dimethyl-1H-pyrazole-carboxylic acid ethyl ester (0.83 g, 5 mM), potassium carbonate (2.07 g, 15 mM), tetrabutylammonium bromide (0.11 g, 0.25 mM), and ethyl bromoacetate (3.32 mL, 5 mM) were mixed in 1,4-dioxane (60 mL). The reaction mixture was stirred at 140 °C for 24 h and the solvent was removed by evaporation. The residue was dissolved in CH₂Cl₂ (40 mL) and washed with deionized water (200 mL). The organic layer was dried over MgSO₄ and evaporated to give 1-ethoxycarbonylmethyl-3,5dimethyl-1H-pyrazole-4-carboxylic acid ethyl ester (Ecmdpcaee) as a faint yellow oil. Yield: 0.78 g (78.7%). ¹H NMR (CDCl₃, 500 MHz) δ: 4.80 (s, 2H), 4.16 (q, 2H), 4.24 (q, 2H), 2.47 (s, 3H), 2.42 (s, 3H), 1.36 (t, 3H), 1.28 (t, 3H); ESI-MS: *m/z* (%) 254.95 [MH⁺] (100%), 274.10[MK⁺] (100%); IR (cm⁻¹, KBr pellet): 3378 (m), 2985

(vs), 2931 (vs), 2587 (w), 1735 (vs), 1702 (s), 1656 (w), 1552 (s), 1447 (m), 1374 (s), 1356 (w), 1282 (s), 1233 (vs), 1160 (w), 1051 (w), 873 (m), 686 (m); m.p.: 50–52 °C.

2.2.2. Synthesis of 1-carboxymethyl-3,5-dimethyl-1H-pyrazole-4-carboxylic acid (H₂cmdpca). 1-Ethoxycarbonylmethyl-3,5-dimethyl-1H-pyrazole-4-carboxylic acid ethyl ester (1.00 g, 3.94 mM) and sodium hydroxide (0.39 g, 10 mM) were mixed in distilled water (100 mL) and stirred at 100 °C for 4 h, then filtered to give a colorless solution. The resulting solution was acidified to pH 3 with 12 M L⁻¹ HCl solution and allowed to stand at low temperature for 2 h, resulting in the production of precipitate. The precipitate was filtered and washed with distilled water, then dried in vacuum to give 1-carboxymethyl-3,5-dimethyl-1H-pyrazole-4-carboxylic acid (H₂cmdpca) as white powder. Yield: 0.308 g (50.6%). Colorless crystals suitable for X-ray diffraction were obtained by volatilizing the mixed solvent of water and dichloromethane (V : V = 1 : 1), corresponding to H₂cmdpca. Anal. Calcd for C₈H₁₀N₂O₄ (%): C, 48.44; H, 5.05; N, 14.13. Found: C, 48.46; H, 5.03; N, 14.11. ¹H NMR (CDCl₃, 500 MHz): δ: 12.67 (s, 2H), 4.88 (s, 2H), 2.38 (s, 3H), 2.26 (s, 3H); ESI-MS: *m/z* (%) 198.9 [MH⁺] (100%); IR (cm⁻¹, KBr pellet): 3559 (s) 3017 (m), 2973 (s), 2922 (w), 2736 (w), 2608 (m), 1730 (s), 1670 (m), 1554 (vs), 1433 (m), 1310 (s), 1242 (vs), 1139 (s), 1041 (w), 930 (m), 881 (m). m.p.: 260.5–264 °C.

2.2.3. Synthesis of [Cd(4,4'-bpy)(Hcmdpca)₂(H₂O)₃]·H₂O (1). A solution of Cd(NO₃)₂·4H₂O (0.1 mM, 0.0308 g) in distilled water (2 mL) was slowly added to a solution of H₂cmdpca (0.2 mM, 0.0396 g) and 4,4'-bpy (0.05 mM, 0.0099 g) in DMF (4 mL) to obtain a colorless solution. The resulting solution was allowed to stand at ambient temperature for some days, giving colorless crystals in 20.8% yield based on Cd. Anal. Calcd for C₂₆H₃₄CdN₆O₁₂ (Mr = 734.99): C, 42.45; H, 4.63; N, 11.43. Found: C, 42.48; H, 4.57; N, 11.46. IR (cm⁻¹, KBr pellet): 3408 (s), 3153 (w), 2679 (w), 2595 (m), 1644 (vs), 1543 (vs), 1502 (s), 1377 (s), 1319 (s), 1217 (s), 1118 (vs), 1068 (w), 926 (m), 817 (w), 776 (m).

2.2.4. Synthesis of [Cd(4,4'-bpy)(Hcmdpca)₂(H₂O)]·3H₂O (2). Synthesis of **2** was similar to that of **1**, but the ratio of Cd(NO₃)₂·4H₂O/H₂cmdpca/4,4'-bpy is 1 : 2 : 1. Colorless crystals of **2** were obtained in 44.0% yield based on Cd. Anal. Calcd for C₂₆H₃₄CdN₆O₁₂ (Mr = 734.99): C, 42.45; H, 4.63; N, 11.43. Found: C, 42.49; H, 4.58; N, 11.42. IR (cm⁻¹, KBr pellet): 3415 (m), 1671 (s), 1608 (s), 1544 (w), 1496 (s), 1377 (s), 1283 (m), 1212 (m), 1132 (s), 1006 (w), 744 (w).

2.2.5. Synthesis of [Cd(4,4'-bpy)(Hcmdpca)₂(H₂O)] (3). Synthesis of **3** was similar to that of **1**, but the ratio of Cd(NO₃)₂·4H₂O/H₂cmdpca/4,4'-bpy is 1 : 1 : 1. Colorless crystals of **3** were obtained in 48.65% yield based on Cd. Anal. Calcd for C₂₆H₂₈CdN₆O₉ (Mr = 680.94): C, 45.86; H, 4.11; N, 12.34. Found: C, 45.87; H, 4.14; N, 12.38. IR (cm⁻¹, KBr pellet): 3413 (m), 2936 (w), 2586 (w), 1678 (s), 1635 (m), 1585 (vs), 1552 (s), 1384 (s), 1290 (s), 1210 (s), 1043 (w), 885 (w), 817 (s), 768 (s), 625 (m).

2.3. X-ray crystallography

Single-crystal X-ray diffraction measurements were carried out with a Bruker Smart Apex CCD area detector at 293(2) ($H_2cmdpca$) and 291(2) K (**1**, **2** and **3**), respectively. Intensities of reflections were measured with graphite-monochromated Mo- K_α radiation ($\lambda = 0.71073 \text{ \AA}$) with the φ - ω scan mode from $1.40^\circ \leq \theta \leq 27.6^\circ$. The structures were solved by direct methods and refined by full-matrix least-squares on F^2 employing SHELXTL-97 [57]. Anisotropic thermal factors were assigned to all non-hydrogen atoms. Hydrogens attached to C were placed geometrically and allowed to ride during subsequent refinement with an isotropic displacement parameter fixed at 1.2 times U_{eq} of the carbon. Hydrogens attached to O from the water were first located in difference Fourier maps and then placed in the calculated sites and included in the refinement. Crystallographic data and experimental details for the four compounds are summarized in table 1, selected bond lengths (\AA) and angles ($^\circ$) are given in table 2, and hydrogen bond distances and angles are presented in table 3.

3. Results and discussion

3.1. Syntheses and IR spectra

The synthetic procedures of 1-ethoxycarbonylmethyl-3,5-dimethyl-1H-pyrazole-4-carboxylic acid ethyl ester ($Ecmdpcae$) and 1-carboxymethyl-3,5-dimethyl-1H-pyrazole-4-carboxylic acid ($H_2cmdpca$) are shown in scheme 1. In a weak alkaline environment, 3,5-dimethyl-1H-pyrazole-4-carboxylic acid ethyl ester was partly deprotonated and reacted with ethyl bromoacetate with the help of tetraethylammonium bromide (phase transfer catalyst: PTC) to obtain $Ecmdpcae$, then $Ecmdpcae$ was hydrolyzed in an aqueous solution of sodium hydroxide to give $H_2cmdpca$. PTC not only improves the reaction rate but also lowers the reaction temperature. Moreover, 1,4-dioxane is an aprotic solvent and has strong solubility for 3,5-dimethyl-1H-pyrazole-4-carboxylic acid ethyl ester, which made the experiment easy. $H_2cmdpca$ is soluble in DMF, methanol, and ethanol.

$Ecmdpcae$ and $H_2cmdpca$ were characterized by 1H NMR, ESI-MS, and infrared spectroscopies (see figures S1–S6 [see online supplemental material at <http://dx.doi.org/10.1080/00958972.2015.1020305>]). For $Ecmdpcae$, the peaks around 2985 – 2931 cm^{-1} are assigned to the stretch of saturated C–H; the strong peaks at 1735 and 1374 cm^{-1} are related to antisymmetric $\nu_{as}(\text{COO}^-)$ and symmetric $\nu_s(\text{COO}^-)$ stretching vibrations, respectively; the peaks at 1656 and 1552 cm^{-1} are attributed to stretching vibrations of C=N and C=C, respectively; the intense bands within 1282 – 1233 cm^{-1} can be ascribed to stretching vibrations of C–N [54]; the peak at 873 cm^{-1} should be the bending vibration of saturated C–H; a moderately strong peak at 3378 cm^{-1} may be assigned to the O–H stretch from adsorbed water molecules. For $H_2cmdpca$, the strong and broad absorptions around 3000 – 3500 cm^{-1} are assigned as O–H stretching vibrations from carboxylic group; the peaks at 2973 – 2922 cm^{-1} are stretching vibrations of saturated C–H; the strong peaks at 1730 and 1310 cm^{-1} are related to antisymmetric $\nu_{as}(\text{COO}^-)$ and symmetric $\nu_s(\text{COO}^-)$ stretching vibrations, respectively; the peaks at 1670 and 1554 cm^{-1} are attributed to stretches of C=N and C=C, respectively; the intense bands at 1242 – 1139 cm^{-1} can be ascribed to the stretching vibrations of C–N, while the peaks at 930 and 881 cm^{-1} are attributed to bending vibrations of O–H and saturated C–H, respectively.

Table 1. Crystal data and structure refinement parameters for H₂cmdpca and 1–3.

Compound	H ₂ cmdpca	1	2	3
Empirical formula	C ₈ H ₁₀ N ₂ O ₄	C ₂₆ H ₃₄ CdN ₆ O ₁₂	C ₂₆ H ₃₄ CdN ₆ O ₁₂	C ₂₆ H ₂₈ CdN ₆ O ₉
Formula weight	198.18	734.99	734.99	680.94
Temperature (K)	293(2)	291(2)	291(2)	291(2)
Wavelength (Å)	0.71073	0.71073	0.71073	0.71073
Crystal system	Monoclinic	Monoclinic	Monoclinic	Monoclinic
Space group	<i>P</i> 2 ₁ / <i>n</i>	<i>P</i> 2 ₁ / <i>c</i>	<i>P</i> 2 ₁ / <i>n</i>	<i>P</i> 2 ₁ / <i>c</i>
<i>a</i> (Å)	4.666(2)	17.5610(12)	15.9783(11)	22.5124(13)
<i>b</i> (Å)	7.297(3)	7.7430(13)	11.8204(16)	14.0935(17)
<i>c</i> (Å)	28.850(13)	25.0396(13)	16.0705(12)	9.0151(11)
α (°)	90	90	90	90
β (°)	90.153(12)	114.797(4)	92.699(3)	100.042(3)
γ (°)	90	90	90	90
Volume (Å ³)	969.8(7)	3090.8(6)	3031.9(5)	2816.5(5)
<i>Z</i> , <i>D</i> _{calc} (g cm ⁻³)	2, 1.357	4, 1.579	4, 1.610	4, 1.606
Mu(Mo K α) (mm ⁻¹)	0.110	0.78	0.79	0.840
<i>F</i> (0 0 0)	416	1504	1504	1384
Crystal size (mm)	0.24 × 0.20 × 0.20	0.25 × 0.22 × 0.20	0.28 × 0.24 × 0.22	0.26 × 0.22 × 0.20
θ range for data collection (°)	1.40–27.6	1.80–26.0	2.5–25.1	1.7–26.0
Index ranges	–6/6, –8/9, –35/25	–22/21, –7/10, –31/32	–19/19, –11/14, –13/19	–17/27, –17/17, –11/11
Total reflections	6120	19,628	17,539	16,802
Unique reflections (<i>R</i> _{int})	2187 (0.048)	7093 (0.035)	5938 (0.010)	5529 (0.013)
Refinement method	Full-matrix least squares on <i>F</i> ²			
Data/restraints/parameters	1716/0/130	7093/0/410	5938/0/409	5529/0/383
Goodness-of-fit on <i>F</i> ²	1.064	1.035	1.040	1.097
<i>R</i> ₁ , <i>wR</i> ₂ [<i>I</i> > 2 σ (<i>I</i>)]	0.0576, 0.1754	0.0564, 0.1570	0.0586, 0.1505	0.0531, 0.1301
<i>R</i> ₁ , <i>wR</i> ₂ (all data)	0.0826, 0.1938	0.0697, 0.1586	0.0598, 0.1508	0.0569, 0.1305
Largest diff. peak and hole (e Å ⁻³)	0.25 and –0.26	0.86 and –0.52	0.63 and –0.67	0.70 and –0.58

Table 2. Selected bond lengths (Å) and angles (°) for H₂cmdpca and 1–3.

H ₂ cmdpca			
O1–C8	1.192(3)	O3–C4	1.264(3)
C2–C3	1.422(3)	N1–C2	1.323(3)
N1–N2	1.371(2)		
N2–C5–C3	106.25(18)	O4–C4–C3	117.9(2)
C2–N1–N2	105.63(15)	C3–C5–C6	131.47(19)
C5–N2–C7	127.79(18)	N1–C2–C3	110.15(17)
O1–C8–C7	122.65(19)	O1–C8–O2	124.4(2)
Complex 1			
Cd1–O8	2.081(3)	Cd1–O4	2.084(4)
Cd1–O2	2.129(4)	Cd1–O1	2.134(4)
Cd1–N1	2.166(5)	Cd1–O3	2.241(4)
O8–Cd1–O4	159.88(17)	O8–Cd1–O2	89.44(13)
O4–Cd1–O2	92.25(14)	O8–Cd1–O1	92.19(14)
O4–Cd1–O1	107.87(17)	O2–Cd1–O1	89.19(13)
O8–Cd1–N1	91.48(15)	O4–Cd1–N1	86.62(15)
O2–Cd1–N1	178.80(14)	O1–Cd1–N1	91.54(15)
O8–Cd1–O3	87.27(13)	O4–Cd1–O3	72.64(16)
O2–Cd1–O3	92.29(13)	O1–Cd1–O3	92.29(13)
O1–Cd1–O3	178.42(13)	N1–Cd1–O3	87.00(14)
Complex 2			
Cd1–N2 ⁱ	2.298 (4)	Cd1–O6	2.245 (3)
Cd1–O1W	2.334 (3)	Cd1–N1	2.282 (3)
N2–Cd1 ⁱⁱ	2.298 (4)	Cd1–O1	2.287 (3)
O6–Cd1–N2 ⁱ	90.56 (14)	O6–Cd1–N1	94.45 (14)
N1–Cd1–N2 ⁱ	165.38 (15)	O6–Cd1–O1	160.82 (11)
O1–Cd1–N2 ⁱ	88.26 (11)	N1–Cd1–O1	91.42 (12)
O6–Cd1–O1W	80.35 (11)	O1–Cd1–O1W	81.55 (10)
N1–Cd1–O1W	88.64 (12)	N2 ⁱ –Cd1–O1W	105.75 (12)
Symmetry codes: i: 1/2 + x, 3/2 – y, –1/2 + z; ii: –1/2 + x, 3/2 – y, 1/2 + z			
Complex 3			
Cd1–O6 ⁱ	2.225(3)	Cd1–O1	2.233(3)
Cd1–O1W	2.275(3)	Cd1–O5	2.281(3)
Cd1–N1	2.307(4)	Cd1–O2 ⁱ	2.324(3)
Cd1 ⁱⁱ –O6	2.225(3)	Cd1 ⁱⁱ –O2	2.324(3)
O6 ⁱ –Cd1–O1	173.11(11)	O6 ⁱ –Cd1–O1W	89.90(11)
O1–Cd1–O1W	94.83(11)	O6 ⁱ –Cd1–O5	85.21(12)
O6 ⁱ –Cd1–N1	91.89(12)	O1–Cd1–N1	90.84(12)
O1W–Cd1–N1	170.20(11)	O5–Cd1–N1	86.26(13)
O6 ⁱ –Cd1–O2 ⁱ	84.34(11)	O1–Cd1–O2 ⁱ	89.73(11)
O1W–Cd1–O2 ⁱ	91.88(11)	O5–Cd1–O2 ⁱ	164.58(11)
N1–Cd1–O2 ⁱ	82.78(12)		
Symmetry codes: i: x, 3/2 – y, 1/2 + z; ii: x, 3/2 – y, –1/2 + z			

During close examination of the synthesis conditions, we found that the molar ratio of metal ion to ligand plays an important role in the assembly process. Complex 1 can be obtained from Cd(NO₃)₂·4H₂O/H₂cmdpca/4,4'-bpy with molar ratios of 1 : 2 : 0.5. When the molar ratio changed into 1 : 2 : 1 and 1 : 1 : 1, complexes 2 and 3 were obtained, respectively, showing the outcome is molar ratio-dependent. Considering the solvent and the amount of metal salt are the same and the difference is only the molar ratio of the ligands, the outcome is ligand concentration-dependent.

1–3 have similar IR spectra (figures S7–S9). The strong and broad peaks around 3000–3500 cm^{–1} are assigned to ν(OH) of water. The strong peaks at 1644 cm^{–1} (1), 1608 cm^{–1}

Table 3. Hydrogen bond distances (Å) and angles (°) for H₂cmdpca and 1–3.

D–H···A	D–H/Å	H–A/Å	D–A/Å	D–H–A/°
H₂cmdpca				
O(2)–H(2)···N(1) ⁱ	0.82	1.95	2.753(3)	165
O(4)–H(4)···O(3) ⁱⁱ	0.88	1.75	2.616(3)	168
C(6)–H(6B)···O(3)	0.96	2.47	2.993(3)	114
C(7)–H(7A)···O(1) ^{iv}	0.97	2.27	3.163(3)	152
C(7)–H(7B)···O(1) ⁱⁱⁱ	0.97	2.35	3.098(3)	133
Complex 1				
O(1W)–H(1A)···N(6) ^{iv}	0.85	2.55	2.997(5)	114
O(1W)–H(1B)···O(9) ^v	0.85	2.19	2.689(5)	117
O(1)–H(1X)···N(2) ⁱⁱ	0.96	2.03	2.799(7)	136
O(1)–H(1Y)···O(1W) ⁱ	0.96	2.31	2.918(5)	121
O(2)–H(2X)···O(5)	0.96	1.87	2.690(5)	142
O(2)–H(2Y)···O(9)	0.96	2.14	2.688(5)	115
O(3)–H(3Y)···O(1W) ⁱⁱⁱ	0.82	2.14	2.715(5)	117
C(1)–H(1)···O(8)	0.93	2.46	3.044(7)	121
C(5)–H(5)···O(4)	0.93	2.50	2.992(7)	113
O(16)–H(16B)···O(7)	0.96	2.35	3.017(7)	126
O(24)–H(24B)···O(11)	0.96	2.59	3.102(7)	113
O(26)–H(26B)···O(10)	0.96	2.48	2.949(7)	110
Symmetry codes: i: $x, 1 + y, 1 + z$; ii: $1 - x, 2 - y, 2 - z$; iii: $x, y, -1 + z$; iv: $x, y, -1 + z$; v: $-x, 1 - y, 1 - z$.				
Complex 2				
O(1W)–H(1Y)···O(8) ⁱⁱ	0.85	2.20	2.673(4)	115
O(2W)–H(2X)···O(4W) ^{vii}	0.85	2.07	2.733(5)	135
O(2W)–H(2Y)···O(6) ^{viii}	0.85	2.09	2.829(5)	146
O(3)–H(3A)···O(3W) ⁱⁱ	0.96	2.29	2.877(5)	119
O(3)–H(3A)···O(4W) ⁱⁱⁱ	0.96	2.56	2.351(5)	140
O(4W)–H(4X)···O(2) ^{iv}	0.85	2.01	2.750(4)	145
O(7)–H(7A)···N(4) ^v	0.96	1.75	2.612(5)	148
C(2)–H(2)···O(1) ^{iv}	0.93	2.46	3.358(5)	163
C(4)–H(4)···O(5) ⁱ	0.93	2.40	3.300(5)	164
C(7)–H(7)···O(1) ^{iv}	0.93	2.47	3.400(5)	176
C(16)–H(16D)···O(3)	0.96	2.40	2.048(6)	125
C(24)–H(24B)···O(7)	0.96	2.54	3.076(6)	115
C(26)–H(26D)···O(8)	0.96	2.27	2.985(6)	131
Symmetry codes: i: $3/2 - x, 1/2 + y, 3/2 - z$; ii: $x, 1 + y, z$; iii: $3/2 - x, -1/2 + y, 3/2 - z$; iv: $3/2 - x, -1/2 + y, 3/2 - z$; v: $2 - x, 1 - y, 1 - z$; vi: $x, -1 + y, z$; vii: $1/2 + x, 1/2 - y, -1/2 + z$; viii: $3/2 - x, -1/2 + y, 1/2 - z$; ix: $3/2 - x, -3/2 + y, 3/2 - z$.				
Complex 3				
O(1W)–H(1W4)···N(2) ⁱⁱⁱ	0.96	2.13	2.803(5)	126
O(1W)–H(1W5)···O(5) ⁱⁱ	0.96	1.92	2.640(4)	130
O(4)–H(4A)···N(4) ^{iv}	0.96	1.76	2.701(5)	167
O(8)–H(8A)···N(5) ^{vi}	0.85	2.62	2.330(6)	131
O(8)–H(8A)···N(6) ^{vi}	0.96	1.90	2.817(6)	160
C(4)–H(4)···O(7) ⁱⁱ	0.93	2.47	3.224(6)	138
C(12)–H(12A)···O(1) ⁱ	0.97	2.24	3.096(5)	147
C(12)–H(12B)···O(3) ^v	0.97	2.25	3.206(5)	170
C(16)–H(16B)···O(4)	0.96	2.42	2.948(5)	114
C(20)–H(20A)···O(8) ^{vii}	0.97	2.50	3.145(6)	124
C(24)–H(24B)···O(7)	0.96	2.19	2.910(7)	130
Symmetry codes: i: $x, 3/2 - y, -1/2 + z$; ii: $x, 3/2 - y, 1/2 + z$; iii: $x, -1 + y, z$; iv: $1 - x, 1/2 + y, 3/2 - z$; v: $1 - x, -1/2 + y, 3/2 - z$; vi: $2 - x, -1/2 + y, 3/2 - z$; vii: $2 - x, 1/2 + y, 3/2 - z$.				

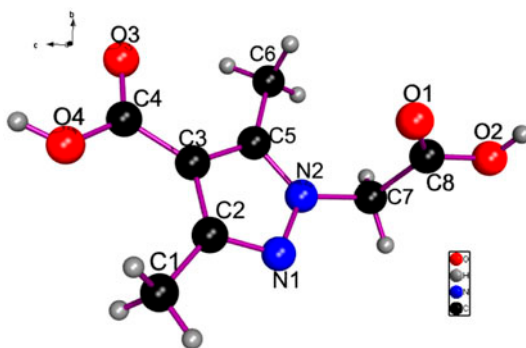


Figure 1. Molecular structure of $H_2cmdpca$.

(2), 1585 cm^{-1} (3), and 1377 cm^{-1} (1), 1377 cm^{-1} (2), 1384 cm^{-1} (3) are assigned to the $\nu_{as}(OCO)$ and $\nu_s(OCO)$ of $Hcmdpca^-$ [58, 59]. Those assignments are supported by the X-ray crystal structure analysis.

3.2. Crystal structures of $H_2cmdpca$, 1, 2, and 3

As shown in figure 1, $H_2cmdpca$ crystallizes in space group $P2_1/n$ with the asymmetric structural unit containing a single $H_2cmdpca$ molecule. The C–O, C–C, and C–N lengths in $H_2cmdpca$ are 1.192–1.264, 1.392–1.505, and 1.323–1.447 Å, respectively, and N–N bond length is 1.371 Å, similar to values seen in $[Co(MPA)_2(H_2O)_2]$ (MPA = 5-methyl-1H-pyrazole-3-carboxylate) [18]. In $H_2cmdpca$, adjacent $H_2cmdpca$ molecules are linked by two kinds of strong hydrogen bonds ($O(2)–H(2)–N(1)^i$, $O(4)–H(4)–O(3)^{ii}$) forming an infinite 2-D structure (figure 2). These 2-D structures are further packed into a 3-D corrugated network via the interaction of other weak hydrogen bonds ($C(6)–H(6B)–O(3)$, $C(7)–H(7A)–O(1)^{iii}$, $C(7)–H(7B)–O(1)^{iiii}$) (table 3), as shown in figure 3.

Complex 1 possesses a mononuclear structure and crystallizes in the monoclinic space group $P2_1/c$. In 1, each Cd(II) is six-coordinate with five oxygens (O1, O2, O3, O4, and

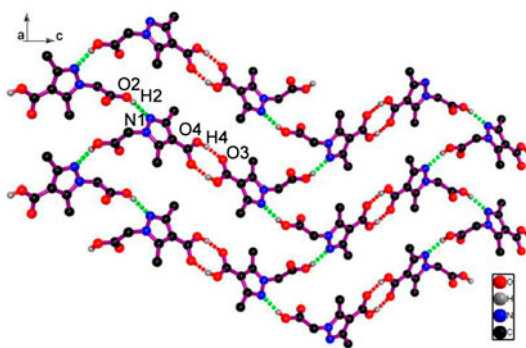


Figure 2. 2-D structure of $H_2cmdpca$ linked by hydrogen bonding interaction. Only hydrogens involved in hydrogen bonds are shown; hydrogen bonds are indicated by dash lines.

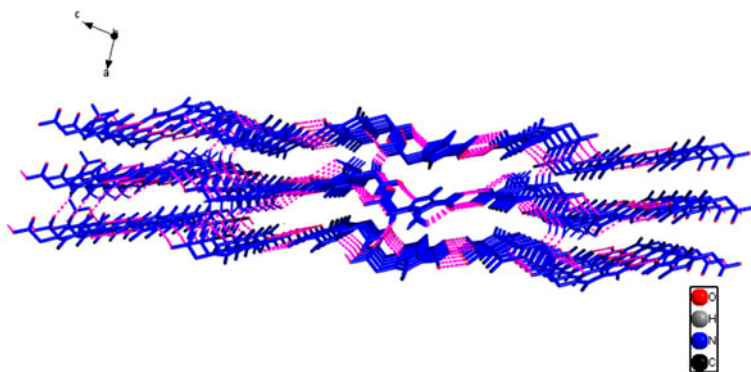


Figure 3. A view of an H-bonded 3-D network of H_2cmdpca down the b axis. Dashed lines represent hydrogen bonds.

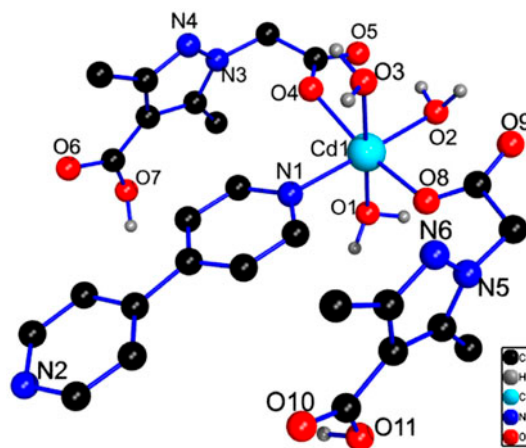


Figure 4. Molecular structure of **1**. Only hydrogens on oxygens are drawn; the others are omitted for clarity.

O5) and one nitrogen (N1) (figure 4). The Cd1–O axial distances are 2.134(4) and 2.241(4) Å, while the equatorial Cd1–O distances are 2.081(3)–2.129(4) Å. The Cd1–N1 distance is 2.166(5) Å, close to those observed in cadmium complexes based on pyrazole derivative ligands [16]. Distortion in octahedral geometry in **1** is reflected in cisoid [72.64(16)–107.87(17)°] and transoid angles [159.88(17)–178.80(14)°] (table 2). The dihedral angle between the 4,4'-bpy ring and the pyrazolyl ring is 68.2°. The separation of 3.692 Å between the centroids of the pyrazolyl ring and the edge of 4,4'-bpy ring indicates significant intramolecular edge to face π – π interactions. Independent components [Cd(4,4'-bpy)(Hcmdpca)₂(H₂O)₃] are linked by three kinds of hydrogen bonds (N–H \cdots O, O–H \cdots O, C–H \cdots O) (table 3), as shown in figure 5, resulting in formation of a 3-D supramolecular architecture with channels. The lattice waters are clathrated in the channels via hydrogen bonds (O(1W)–H(1A) \cdots N(6)^{iv}, O(1)–H(1Y) \cdots O(1W)ⁱ, and O(3)–H(3Y) \cdots O(1W)ⁱⁱⁱ), while the intermolecular π – π interactions between pyrazolyl rings and between 4,4'-bpy molecules

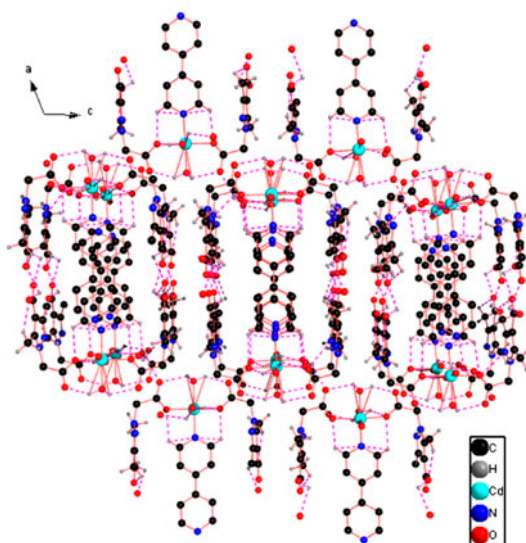


Figure 5. 3-D network of **1** constructed by hydrogen bonding. Broken lines represent hydrogen bonding interactions.

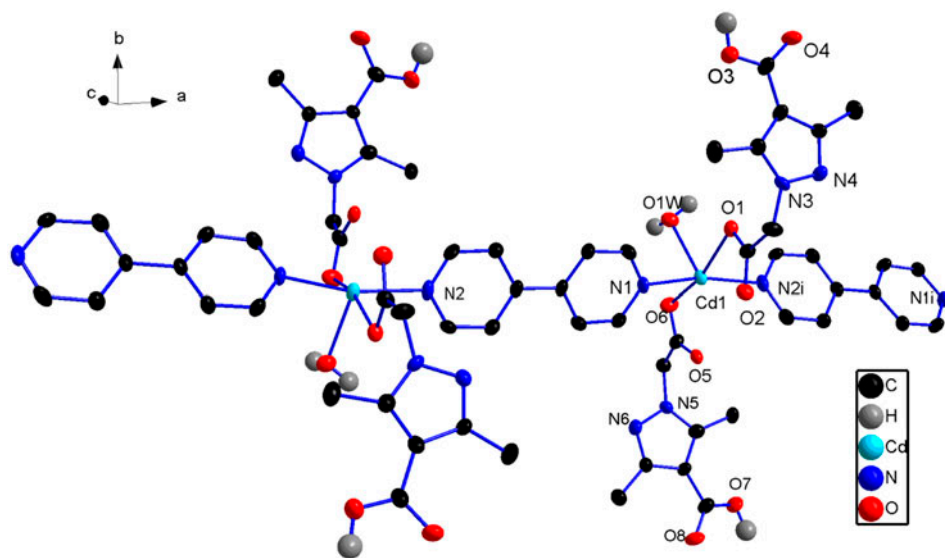


Figure 6. 1-D chain structure of **2**. Only hydrogens on oxygens are drawn; the others are omitted for clarity.

(centroid–centroid distances are 3.596–3.655 Å) further increase the stability of the structure.

Complex **2** crystallizes in the monoclinic space group $P2_1/n$. The asymmetric unit of **2** contains one Cd(II), two Hcndmpca[−] ligands, one 4,4'-bpy, and one coordinated water. As shown in figure 6, Cd(II) is five-coordinate, with two oxygens (O1, O6) from two

carboxylate groups of two Hcmdpca^- ligands, one oxygen (O1W) from a coordinated water molecule, and two nitrogens (N1, N2i) from two 4,4'-bpy, leading to a square-pyramidal coordination geometry. Two nitrogens and two oxygens (N2i, N1, O1, O6) form the plane of the square pyramidal structure and O1 W occupies the apical position. N2i, N1, O1, and O6, and Cd(II) deviate 0.3285 and 0.0422 Å from the base plane, respectively. The bond distances of Cd1–O and Cd1–N, respectively, are 2.245–2.334 and 2.282–2.298 Å (table 2), close to the values observed in other Cd(II) complexes [16]. The bond angles of N2i–Cd1–N1, N2i–Cd1–O1 W, and N1–Cd1–O6 are 165.38(15), 105.75(12), and 94.45(14)°, respectively.

Adjacent Cd(II) ions are linked by one 4,4'-bpy to form a 1-D chain structure, as shown in figure 6. The distance between two Cd(II) ions is 11.623 Å. These 1-D chains and free water molecules are linked by multiple hydrogen bonds (N–H···O, O–H···O, C–H···O) (table 3), as shown in figure 7, resulting in the formation of a 3-D supramolecular microporous architecture. The total potential solvent volume is 347.8 Å³, accounting for ca. 11.5% of cell volume of 3031.9(5) Å³ calculated by the Platon programs.

Compound **3** crystallizes in the monoclinic space group $P2_1/c$. The asymmetric unit of **3** contains one Cd(II), two Hcmdpca^- , one 4,4'-bpy molecule, and one coordinated water molecule. As illustrated in figure 8, the Cd(II) ion is six-coordinate surrounded by five oxygens (O1i, O2, O5, O6i, and O1W) from four Hcmdpca^- ligands and one water, respectively, and the remaining position is occupied by N1 from 4,4'-bpy, forming a distorted octahedron. The Cd–N bond length is 2.307(14) Å and Cd–O bond lengths are 2.225(3)–2.324(3) Å, which are close to the values observed in **2**. The bond angles around Cd(II) are 82.78(12)–173.11(11)°.

Different from coordination mode of Hcmdpca^- in **1** and **2**, as shown in figure 9, each Hcmdpca^- in **3** is bridged to two adjacent Cd(II) ions via deprotonated carboxyl group in bi-monodentate mode, resulting in formation of a $\{\text{Cd}_2(\text{COO})_2\}$ binuclear loop. These

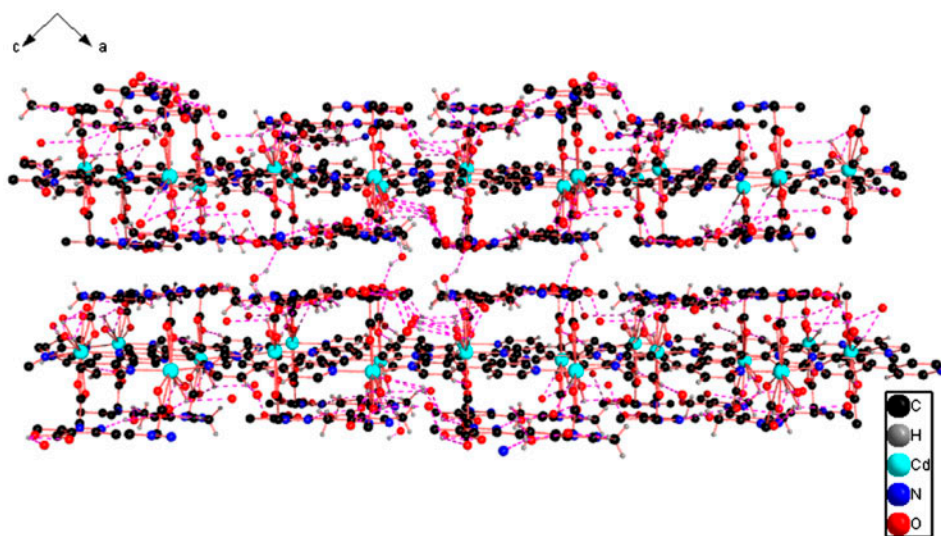


Figure 7. 3-D framework of **2** constructed by hydrogen bonding. Broken lines represent hydrogen bonding interactions.

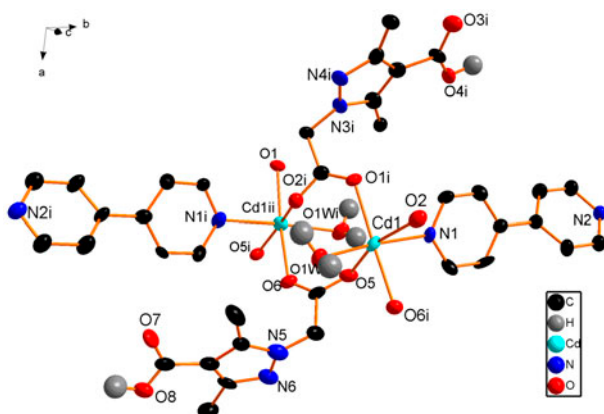


Figure 8. A view of the coordination environment around Cd(II) in **3**. Only hydrogens on oxygens are drawn, with others omitted for clarity.

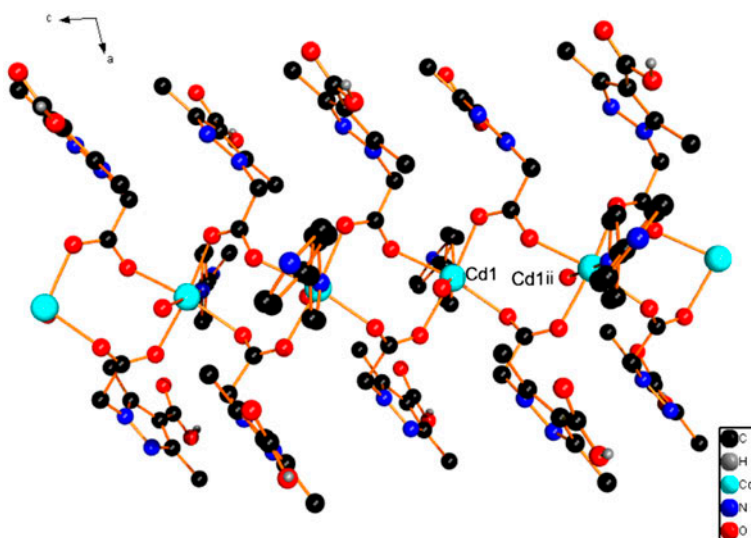


Figure 9. 1-D chain structure of **3** along the *c* axis. Only hydrogens on oxygens are drawn.

$\{\text{Cd}_2(\text{COO})_2\}$ binuclear loops are linked to further form a 1-D chain. The Cd–Cd distance is 4.6884(7) Å. These 1-D chains are assembled into a 3-D supramolecular structure by interactions of N–H \cdots O, O–H \cdots O, and C–H \cdots O hydrogen bonds (table 3), as shown in figure 10.

Complex **2** contains uncoordinated carboxyl groups (free carboxylic acids), while **1** and **3** not only have uncoordinated carboxyl groups but also uncoordinated nitrogens from 4,4'-bpy molecules. These uncoordinated carboxyl groups/nitrogens might serve as Lewis acid/base sites in catalytic and acid–base reactions [60, 61].

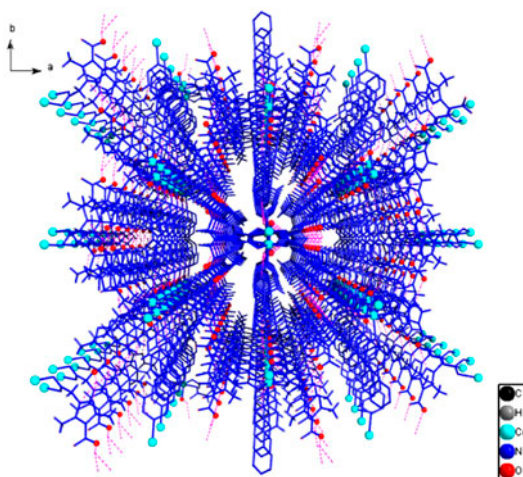


Figure 10. 3-D framework of **3**. Only hydrogens involved in hydrogen bonds are shown; dashed lines represent hydrogen bonds.

3.3. Supramolecular isomerism

From the crystal engineering point of view, **1**, **2**, and **3** are supramolecular isomers because they have same compositions: Cd(II) ion, 4,4'-bpy, and Hcmdpca⁻ anion, and the ratios of the three compositions are all the same (1 : 1 : 2). **1** and **2** have the same stoichiometry for all components, but the coordination environment of Cd(II) in **2** is different from that of Cd(II) in **1**, which are two true supramolecular isomers; compounds **2** and **3** have the same building blocks, [Cd(4,4'-bpy)(Hcmdpca)₂(H₂O)], but different network superstructures and crystalline water molecules. **2** has three crystalline water molecules, while **3** has no crystalline water. **2** and **3** can be related as “pseudo-supramolecular” isomers. The structures of **1–3** are controlled by the concentration of the ligand based on the synthetic conditions; these supramolecular isomers are ligand concentration-dependent.

3.4. Thermal analysis

For detecting the thermal stabilities of **1–3**, thermal gravimetric (TG) analyses were carried out from room temperature to 850 °C in a nitrogen atmosphere (see figure S10, supporting material). The initial weight loss of **1** from 30 to 161 °C, **2** from 50 to 159 °C, and **3** from 105 to 173 °C corresponds to the loss of four, four, and one water molecule, respectively (for **1**, calculated, 9.8%; found, 10.0%; for **2**, calculated, 9.8%; found, 9.6%; for **3**, calculated, 2.60%; found, 2.59%). Subsequently, the remaining materials of **1–3** all decompose gradually.

3.5. Luminescent properties

Luminescent compounds are of interest because of applications in chemical sensors, photochemistry, and electroluminescent display. The photoluminescent behaviors of **1–3**,

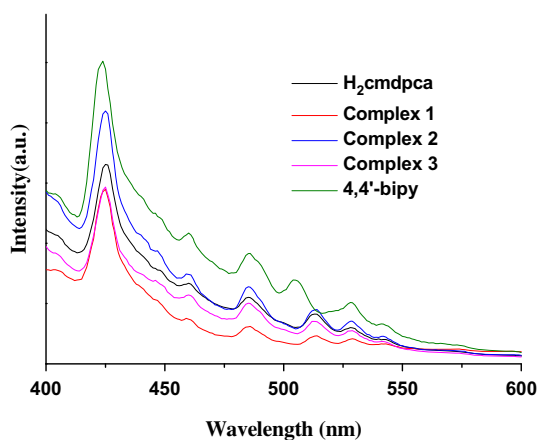


Figure 11. Solid-state emission spectra for 4,4'-bpy, H₂cmdpca, **1**, **2**, and **3** (excitation wavelength = 370 nm) at room temperature.

H₂cmdpca, and 4,4'-bpy are studied in the solid state at room temperature. The excitation and emission spectra are displayed in figure S11 and figure 11, respectively. As illustrated in figure 11, the blue emission for H₂cmdpca, 4,4'-bpy, and **1–3** can be observed, where their maximum emission wavelengths are all at 425 nm. Apparently, the main emission peaks of **1–3** are similar to that of the ligand H₂cmdpca and 4,4'-bpy in terms of the position and the band shape, indicating that the emission bands of **1–3** may be attributed to the emission of intraligand $\pi-\pi^*/n-\pi^*$ transitions [60, 62]. The weaker shoulder peaks of the emission spectra at 460, 485, and 512 nm can probably be assigned to the intraligand transition because similar peaks also appear for the ligands.

4. Conclusion

We have synthesized a new pyrazole carboxylic acid ligand. Three Cadmium(II) supramolecular isomers based on H₂cmdpca have been synthesized and characterized. Complex **1** has mononuclear structure, **2** and **3** show different 1-D structures; the structures are controlled by the concentration of the ligand. **1** and **2** are true supramolecular isomers, while **2** and **3** are “pseudo-supramolecular” isomers. To the best of our knowledge, this is the first example to obtain both true and “pseudo-supramolecular” isomers only by adjusting the concentration of the ligand. The intermolecular hydrogen bond and $\pi-\pi$ interactions play important roles in formation of 3-D supramolecular architectures of **1–3**. The complexes all display ligand-based blue luminescence in the solid state.

Supplementary material

NMR and MS spectra of Ecmdpcaee and H₂cmdpca, IR spectra of Ecmdpcaee, H₂cmdpca, complexes **1–3**, TG curves of complexes **1–3**. Crystallographic data (excluding structure factors) for the structures in this paper have been deposited with the

Cambridge Crystallographic Data Center, 12 Union Road, Cambridge CB2 1EZ. Copies of the data can be obtained by quoting the depository numbers CCDC-963359 (H₂cnd-pca), CCDC-979481 (1), CCDC-979483 (2) and CCDC-979482 (3) (Fax: +44 1223 336 033; E-mail: deposit@ccdc.cam.ac.uk).

Funding

This work was supported by National Natural Science Foundation of China [grant number 20971060], [grant number 21101018]; the Priority Academic Program Development of Jiangsu Higher Education Institutions and the Natural Science Foundation of State Key Laboratory of Coordination Chemistry.

References

- [1] M. O'Keeffe, O.M. Yaghi. *Chem. Rev.*, **112**, 675 (2012).
- [2] G. Férey. *Chem. Soc. Rev.*, **37**, 191 (2008).
- [3] K. Ohara, M. Kawano, Y. Inokuma, M. Fujita. *J. Am. Chem. Soc.*, **132**, 30 (2010).
- [4] L.Q. Ma, C. Abney, W.B. Lin. *Chem. Soc. Rev.*, **38**, 1248 (2009).
- [5] M. Dincă, J.R. Long. *Angew. Chem. Int. Ed.*, **47**, 6766 (2008).
- [6] H. Deng, C.J. Doonan, H. Furukawa, R.B. Ferreira, J. Towne, C.B. Knobler, B. Wang, O.M. Yaghi. *Science*, **327**, 846 (2010).
- [7] B. Wang, A.P. Côté, H. Furukawa, M. O'Keeffe, O.M. Yaghi. *Nature*, **453**, 207 (2008).
- [8] J.R. Li, J. Sculley, H.C. Zhou. *Chem. Rev.*, **112**, 869 (2012).
- [9] O.S. Wenger. *Chem. Rev.*, **113**, 3686 (2013).
- [10] Q. Liu, L.L. Yu, Y. Wang, Y.Z. Ji, J. Horvat, M.L. Cheng, X.Y. Jia, G.X. Wang. *Inorg. Chem.*, **52**, 2817 (2013).
- [11] G. Férey, F. Millange, M. Morcrette, C. Serre, M.-L. Doublet, J.-M. Grenèche, J.-M. Tarascon. *Angew. Chem. Int. Ed.*, **46**, 3259 (2007).
- [12] M. Nagarathinam, K. Saravanan, E.J.H. Phua, M.V. Reddy, B.V.R. Chowdari, J.J. Vittal. *Angew. Chem.*, **124**, 5968 (2012).
- [13] X. Zhu, J.W. Zhao, B.L. Li, Y. Song, Y.M. Zhang, Y. Zhang. *Inorg. Chem.*, **49**, 1266 (2010).
- [14] Y.J. Cui, Y.F. Yue, G.D. Qian, B.L. Chen. *Chem. Rev.*, **112**, 1126 (2012).
- [15] M.X. Yao, Q. Zheng, X.M. Cai, Y.Z. Li, Y. Song, J.L. Zuo. *Inorg. Chem.*, **51**, 2140 (2012).
- [16] L.T. Chen, F. Tao, L.D. Wang, J. Hong, X.Y. Jia, J.T. Bao, Y.Z. Ji, M.L. Cheng, Q. Liu. *Z. Anorg. Allg. Chem.*, **639**, 552 (2013).
- [17] L.D. Wang, F. Tao, M.L. Cheng, Q. Liu, W. Han, Y.J. Wu, D.D. Yang, L.J. Wang. *J. Coord. Chem.*, **65**, 923 (2012).
- [18] W. Han, M.L. Cheng, Q. Liu, L.D. Wang, Y.J. Wu. *Chin. J. Inorg. Chem.*, **28**, 1997 (2012).
- [19] J.T. Bao, M.L. Cheng, Q. Liu, W. Han, C.W. Zhai, J. Hong, X.Q. Sun. *Chin. J. Inorg. Chem.*, **29**, 1504 (2013).
- [20] M.L. Cheng, W. Han, Q. Liu, J. Bao, Z. Li, L. Chen, X.Q. Sun, H. Xi. *J. Coord. Chem.*, **67**, 215 (2014).
- [21] X.H. Zhou, X.D. Du, G.N. Li, J.L. Zuo, X.Z. You. *Cryst. Growth Des.*, **9**, 4487 (2009).
- [22] J. Lincke, D. Lässig, M. Kobalz, J. Bergmann, M. Handke, J. Möllmer, M. Lange, C. Roth, A. Möller, R. Staudt, H. Krautscheid. *Inorg. Chem.*, **51**, 7579 (2012).
- [23] L. Pan, T. Frydel, M.B. Sander, X. Huang, J. Li. *Inorg. Chem.*, **40**, 1271 (2001).
- [24] C. Montoro, F. Linares, E. Quartapelle Procopio, I. Senkovska, S. Kaskel, S. Galli, N. Masciocchi, E. Barea, J.A.R. Navarro. *J. Am. Chem. Soc.*, **133**, 11888 (2011).
- [25] E. Quartapelle Procopio, T. Fukushima, E. Barea, J.A.R. Navarro, S. Horike, S. Kitagawa. *Chem. Eur. J.*, **18**, 13117 (2012).
- [26] C. Heering, I. Boldog, V. Vasylyeva, J. Sanchiz, C. Janiak. *CrystEngComm*, **15**, 9757 (2013).
- [27] X.L. Qi, C. Zhang, B.Y. Wang, W. Xue, C.T. He, S.Y. Liu, W.X. Zhang, X.M. Chen. *CrystEngComm*, **15**, 9530 (2013).
- [28] R.Q. Fang, X.M. Zhang. *Inorg. Chem.*, **45**, 4801 (2006).
- [29] B. Moulton, M.J. Zaworotko. *Chem. Rev.*, **101**, 1629 (2001).
- [30] J.P. Zhang, X.C. Huang, X.M. Chen. *Chem. Soc. Rev.*, **38**, 2385 (2009).
- [31] S.R. Batten, R. Robson. *Angew. Chem.*, **110**, 1558 (1998); *Angew. Chem. Int. Ed.*, **37**, 1460 (1998).
- [32] A.J. Blake, N.R. Brooks, N.R. Champness, M. Crew, A. Deveson, D. Fenske, D.H. Gregory, L.R. Hanton, P. Hubberstey, M. Schroder. *Chem. Commun.*, 1432, (2001).
- [33] L. Jiang, T.B. Lu, X.L. Feng. *Inorg. Chem.*, **44**, 7056 (2005).
- [34] X.C. Huang, J.P. Zhang, X.M. Chen. *J. Am. Chem. Soc.*, **126**, 13218 (2004).

- [35] Y. Gao, J.Z. Liu, C.W. Hu, W.L. Gao. *Inorg. Chem. Commun.*, **10**, 575 (2007).
- [36] P.A. Gale, M.E. Light, R. Quesada. *Chem. Commun.*, 5864, (2005).
- [37] L. Carlucci, G. Ciani, S. Maggini, D.M. Proserpio. *Cryst. Growth Des.*, **8**, 162 (2008).
- [38] Y.S. Tan, A.L. Sudlow, K.C. Molloy, Y. Morishima, K. Fujisawa, W.J. Jackson, W. Henderson, S.N.B.A. Halim, S.W. Ng, E.R.T. Tiekink. *Cryst. Growth Des.*, **13**, 3046 (2013).
- [39] M.D. Zhang, L. Qin, H.T. Yang, Y.Z. Li, Z.J. Guo, H.G. Zheng. *Cryst. Growth Des.*, **13**, 1961 (2013).
- [40] Y. Wang, C.T. He, Y.J. Liu, T.Q. Zhao, X.M. Lu, W.X. Zhang, J.P. Zhang, X.M. Chen. *Inorg. Chem.*, **51**, 4772 (2012).
- [41] Z. Yan, Z.P. Ni, F.S. Guo, J.Y. Li, Y.C. Chen, J.L. Liu, W.Q. Lin, D. Aravena, E. Ruiz, M.L. Tong. *Inorg. Chem.*, **53**, 201 (2014).
- [42] Y.X. Hu, H.B. Ma, B. Zheng, W.W. Zhang, S. Xiang, L. Zhai, L.F. Wang, B. Chen, X.M. Ren, J. Bai. *Inorg. Chem.*, **51**, 7066 (2012).
- [43] S. Masaoka, D. Tanaka, Y. Nakanishi, S. Kitagawa. *Angew. Chem., Int. Ed.*, **43**, 2530 (2004).
- [44] X.C. Huang, J.P. Zhang, Y.Y. Lin, X.M. Chen. *Chem. Commun.*, 2232, (2005).
- [45] M.L. Tong, S. Hu, J. Wang, S. Kitagawa, S.W. Ng. *Cryst. Growth Des.*, **5**, 837 (2005).
- [46] M.H. Bi, G.H. Li, J. Hua, Y.L. Liu, X.M. Liu, Y.W. Hu, Z. Shi, S.H. Feng. *Cryst. Growth Des.*, **7**, 2066 (2007).
- [47] Z.G. Li, G.H. Wang, H.Q. Jia, N.H. Hu, J.W. Xu. *CrystEngComm*, **9**, 882 (2007).
- [48] Z.M. Hao, X.M. Zhang. *Cryst. Growth Des.*, **7**, 64 (2007).
- [49] P. Kanoo, K.L. Gurunatha, T.K. Maji. *Cryst. Growth Des.*, **9**, 4147 (2009).
- [50] S.Z. Zhan, D. Li, X.P. Zhou, X.H. Zhou. *Inorg. Chem.*, **45**, 9163 (2006).
- [51] K.M. Fromm, J.L.S. Doimeadios, A.Y. Robin. *Chem. Commun.*, 4548, (2005).
- [52] P.X. Yin, J. Zhang, Z.J. Li, Y.Y. Qin, J.K. Cheng, L. Zhang, Q.P. Lin, Y.G. Yao. *Cryst. Growth Des.*, **9**, 4884 (2009).
- [53] S. Wang, H. Zang, C. Sun, G. Xu, X. Wang, K. Shao, Y. Lan, Z. Su. *CrystEngComm*, **12**, 3458 (2010).
- [54] C.P. Li, J.M. Wu, M. Du. *Inorg. Chem.*, **50**, 9284 (2011).
- [55] Y. Jia, H. Li, Q. Guo, B. Zhao, Y. Zhao, H. Hou, Y. Fan. *Eur. J. Inorg. Chem.*, **2012**, 3047 (2012).
- [56] S.I. Yakimovich, I.V. Zerova, V.V. Pakal'nis. *Russ. J. Org. Chem.*, **625**, 44 (2008).
- [57] G.M. Sheldrick. *SHELXTL-9, Program for X-ray Crystal Structure Determination*, University of Göttingen, Göttingen, Germany (1997).
- [58] P. Mahata, S. Natarajan. *Eur. J. Inorg. Chem.*, **11**, 2156 (2005).
- [59] J. Hong, M. Cheng, Q. Liu, W. Han, Y. Zhang, Y. Ji, X. Jia, Z. Li. *Transition Met. Chem.*, **38**, 385 (2013).
- [60] S. Su, M. Cheng, Y. Ren, C. Zhai, F. Tao, Q. Liu. *Transition Met. Chem.*, **39**, 559 (2014).
- [61] B. Chen, L. Wang, Y. Xiao, F.R. Fronczek, M. Xue, Y. Cui, G.D. Qian. *Angew. Chem. Int. Ed.*, **48**, 500 (2009).
- [62] X. Zhu, Q. Chen, Z. Yang, B.L. Li, H.Y. Li. *CrystEngComm*, **15**, 471 (2013).